

Competition of Fermi surface symmetry breaking and superconductivity

Hiroyuki Yamase and Walter Metzner

Max-Planck-Institute for Solid State Research, D-70569 Stuttgart, Germany

(Dated: September 20, 2018)

We analyze a mean-field model of electrons on a square lattice with two types of interaction: forward scattering favoring a d -wave Pomeranchuk instability and a BCS pairing interaction driving d -wave superconductivity. Tuning the interaction parameters a rich variety of phase diagrams is obtained. If the BCS interaction is not too strong, Fermi surface symmetry breaking is stabilized around van Hove filling, and coexists with superconductivity at low temperatures. For pure forward scattering Fermi surface symmetry breaking occurs typically via a first order transition at low temperatures. The presence of superconductivity reduces the first order character of this transition and, if strong enough, can turn it into a continuous one. This gives rise to a quantum critical point within the superconducting phase. The superconducting gap tends to suppress Fermi surface symmetry breaking. For a relatively strong BCS interaction, Fermi surface symmetry breaking can be limited to intermediate temperatures, or can be suppressed completely by pairing.

PACS: 71.10.Fd, 71.10.Pm, 74.20.Mn

I. INTRODUCTION

Usually the Fermi surface of an interacting electron systems respects the point-group symmetry of the underlying crystal lattice. However, electron-electron interactions may also lead to Fermi surface deformations which break the orientational symmetry spontaneously. From a Fermi liquid viewpoint this can happen via a “Pomeranchuk instability”, that is, when Pomeranchuk’s stability condition¹ for the forward scattering interactions is violated.

Interactions favoring a symmetry-breaking Fermi surface deformation with a d -wave order parameter, where the surface expands along the k_x -axis and shrinks along the k_y -axis (or vice versa), are present in the t - J ,² Hubbard,^{3,4} and extended Hubbard⁵ model on a square lattice. These models therefore exhibit enhanced “nematic” correlations, which also appear in the context of fluctuating stripe order.⁶ Signatures for such correlations have been observed in various cuprate superconductors.⁷ In particular, they provide a natural explanation for the relatively strong in-plane anisotropy observed in the magnetic excitation spectrum of $\text{YBa}_2\text{Cu}_3\text{O}_y$.^{8,9}

Fermi surface symmetry breaking competes with superconductivity. In the t - J model

the d -wave Fermi surface deformation instability is overwhelmed by d -wave pairing. This is indicated by slave-boson mean-field theory² and has been confirmed recently by a variational Monte Carlo calculation.¹⁰ However, enhanced nematic correlations remain.¹¹ The competition of superconductivity and Fermi surface symmetry breaking is more delicate in the two-dimensional Hubbard model. Renormalization group calculations in the symmetric phase suggest that the superconducting instability is always stronger than the Pomeranchuk instability,¹² but these calculations do not exclude the possibility of *coexistence* of the two competing order parameters in the symmetry-broken phase. Indeed, coexistence of d -wave superconductivity and d -wave Fermi surface symmetry breaking has been obtained near van Hove filling from a weak coupling perturbation expansion for the symmetry-broken ground state of the Hubbard model.¹³

To elucidate the interplay and competition of Fermi surface symmetry breaking and superconductivity in a more general setting, and to classify possible scenarios, we analyze in the present work a mean-field model allowing for both instabilities with a tunable strength for each. The model describes itinerant electrons on a square lattice with two types of interaction: a reduced BCS interaction driving d -wave superconductivity and a purely forward scattering interaction driving d -wave Fermi surface symmetry breaking.

The properties of the mean-field model without BCS interaction, where the electrons interact only via forward scattering (“f-model”), have been clarified already earlier.^{14,15,16} The main results can be summarized as follows. Fermi surface symmetry-breaking occurs below a transition temperature T_c which forms a dome-shaped line as a function of the chemical potential μ , with a maximal T_c near van Hove filling.^{14,15} The phase transition is usually first order at the edges of the transition line, and always second order around its center.^{14,15,16} The d -wave compressibility of the Fermi surface is however strongly enhanced even near the first order transition down to zero temperature.¹⁶ Adding a uniform repulsion to the forward scattering interaction, the two tricritical points at the ends of the second order transition line are shifted to lower temperatures. For a favorable choice of hopping and interaction parameters one of the first order edges can be replaced completely by a second order transition line, leading to a quantum critical point.¹⁶ Fluctuations at and near the quantum critical point destroy fermionic quasi-particle excitations, leading to non-Fermi liquid behavior.^{17,18}

Adding an attractive d -wave BCS interaction to the f-model leads to a variety of qualitatively distinct phase diagrams, depending on the interaction strength. If the BCS interaction is not too strong, Fermi surface symmetry breaking is stabilized around van Hove filling, and coexists with superconductivity at low temperatures. In the presence of a pairing gap it is easier to realize Fermi surface symmetry breaking via a continuous phase transition at low temperatures than without. In particular, a quantum critical point connecting superconducting phases with and without Fermi surface symmetry breaking at zero temperature is obtained for a suitable choice of interactions. For a relatively

strong BCS interaction, Fermi surface symmetry breaking can be limited to intermediate temperatures, or can be suppressed completely by pairing.

The article is structured as follows. In Sec. II we introduce the mean-field model and describe the self-consistency equations for the order parameters. The phase diagrams and other results are presented in Sec. III. A conclusion follows in Sec. IV.

II. MEAN-FIELD MODEL

We analyze itinerant electrons on a square lattice interacting via forward scattering and a reduced BCS interaction, described by a Hamiltonian of the form

$$H = \sum_{\mathbf{k}} \epsilon_{\mathbf{k}}^0 n_{\mathbf{k}} + H_I^f + H_I^c, \quad (1)$$

where $n_{\mathbf{k}} = \sum_{\sigma} n_{\mathbf{k}\sigma}$ counts the spin-summed number of electrons with momentum \mathbf{k} . The kinetic energy is due to hopping between nearest and next-nearest neighbors on a square lattice, leading to the bare dispersion relation

$$\epsilon_{\mathbf{k}}^0 = -2t(\cos k_x + \cos k_y) - 4t' \cos k_x \cos k_y. \quad (2)$$

The forward scattering interaction reads

$$H_I^f = \frac{1}{2L} \sum_{\mathbf{k}, \mathbf{k}'} f_{\mathbf{k}\mathbf{k}'} n_{\mathbf{k}} n_{\mathbf{k}'}, \quad (3)$$

where L is the number of lattice sites, and the function $f_{\mathbf{k}\mathbf{k}'}$ has the form

$$f_{\mathbf{k}\mathbf{k}'} = u - g_f d_{\mathbf{k}} d_{\mathbf{k}'}, \quad (4)$$

with coupling constants $u \geq 0$ and $g_f \geq 0$, and a function $d_{\mathbf{k}}$ with $d_{x^2-y^2}$ -wave symmetry such as $d_{\mathbf{k}} = \cos k_x - \cos k_y$. This ansatz mimics the structure of the effective interaction in the forward scattering channel as obtained for the t - J^2 and Hubbard³ model. The uniform term originates directly from the repulsion between electrons and suppresses the (uniform) electronic compressibility of the system. The d -wave term enhances the d -wave compressibility and drives spontaneous Fermi surface symmetry breaking. In the Hubbard model it is generated by fluctuations, while in the t - J model the nearest neighbor interaction contributes directly to a d -wave attraction in the forward scattering channel.

The BCS interaction has the form

$$H_I^c = \frac{1}{L} \sum_{\mathbf{k}, \mathbf{k}'} V_{\mathbf{k}\mathbf{k}'} c_{\mathbf{k}\uparrow}^{\dagger} c_{-\mathbf{k}\downarrow}^{\dagger} c_{-\mathbf{k}'\downarrow} c_{\mathbf{k}'\uparrow}. \quad (5)$$

It is a reduced interaction in the sense that it contributes only in the Cooper channel, that is, when the total momentum of the interacting particles vanishes. For the matrix element $V_{\mathbf{k}\mathbf{k}'}$ we choose a separable d -wave attraction

$$V_{\mathbf{k}\mathbf{k}'} = -g_c d_{\mathbf{k}} d_{\mathbf{k}'} \quad (6)$$

with $g_c \geq 0$, which corresponds to the dominant term in the Cooper channel for the two-dimensional Hubbard and t - J model.

Inserting $n_{\mathbf{k}} = \langle n_{\mathbf{k}} \rangle + \delta n_{\mathbf{k}}$ into H_I^f , and $c_{\mathbf{k}\uparrow}^\dagger c_{-\mathbf{k}\downarrow}^\dagger = \langle c_{\mathbf{k}\uparrow}^\dagger c_{-\mathbf{k}\downarrow}^\dagger \rangle + \delta(c_{\mathbf{k}\uparrow}^\dagger c_{-\mathbf{k}\downarrow}^\dagger)$ into H_I^c , and neglecting terms quadratic in the fluctuations, one obtains the mean-field Hamiltonian

$$H_{\text{MF}} = \sum_{\mathbf{k}} \left[\epsilon_{\mathbf{k}} n_{\mathbf{k}} + (\Delta_{\mathbf{k}} c_{\mathbf{k}\uparrow}^\dagger c_{-\mathbf{k}\downarrow}^\dagger + h.c.) - \frac{\delta \epsilon_{\mathbf{k}}}{2} \langle n_{\mathbf{k}} \rangle - \Delta_{\mathbf{k}} \langle c_{\mathbf{k}\uparrow}^\dagger c_{-\mathbf{k}\downarrow}^\dagger \rangle \right]. \quad (7)$$

Here $\epsilon_{\mathbf{k}} = \epsilon_{\mathbf{k}}^0 + \delta \epsilon_{\mathbf{k}}$ is a renormalized dispersion relation, which is shifted with respect to the bare dispersion by $\delta \epsilon_{\mathbf{k}} = L^{-1} \sum_{\mathbf{k}'} f_{\mathbf{k}\mathbf{k}'} \langle n_{\mathbf{k}'} \rangle = un + \eta d_{\mathbf{k}}$, where $n = L^{-1} \sum_{\mathbf{k}} \langle n_{\mathbf{k}} \rangle$ is the average particle density, and

$$\eta = -\frac{g_f}{L} \sum_{\mathbf{k}} d_{\mathbf{k}} \langle n_{\mathbf{k}} \rangle \quad (8)$$

is our order parameter for Fermi surface symmetry breaking. It vanishes as long as the momentum distribution function $\langle n_{\mathbf{k}} \rangle$ respects the symmetry of the square lattice. The superconducting gap function is given by $\Delta_{\mathbf{k}} = \frac{1}{L} \sum_{\mathbf{k}'} V_{\mathbf{k}\mathbf{k}'} \langle c_{-\mathbf{k}'\downarrow} c_{\mathbf{k}'\uparrow} \rangle = \Delta d_{\mathbf{k}}$, where

$$\Delta = -\frac{g_c}{L} \sum_{\mathbf{k}} d_{\mathbf{k}} \langle c_{-\mathbf{k}\downarrow} c_{\mathbf{k}\uparrow} \rangle. \quad (9)$$

For the reduced interactions H_I^f and H_I^c the mean-field decoupling is exact in the thermodynamic limit. Feynman diagrams describing contributions beyond mean-field theory have zero measure for $L \rightarrow \infty$.

The mean-field Hamiltonian is quadratic in the Fermi operators and can be diagonalized by a Bogoliubov transformation. For the grand canonical potential per lattice site, $\omega = L^{-1}\Omega$, we obtain

$$\omega(\eta, \Delta) = -\frac{2}{\beta L} \sum_{\mathbf{k}} \log[2 \cosh(\beta E_{\mathbf{k}}/2)] + \frac{\eta^2}{2g_f} + \frac{|\Delta|^2}{g_c} + un - \frac{un^2}{2} - \mu, \quad (10)$$

where β is the inverse temperature, $E_{\mathbf{k}} = (\xi_{\mathbf{k}}^2 + |\Delta_{\mathbf{k}}|^2)^{1/2}$, and $\xi_{\mathbf{k}} = \epsilon_{\mathbf{k}} - \mu$. The stationarity conditions $\partial\omega/\partial\eta = 0$ and $\partial\omega/\partial\Delta = 0$ yield the self-consistency equations for the order parameters

$$\eta = \frac{g_f}{L} \sum_{\mathbf{k}} d_{\mathbf{k}} \frac{\xi_{\mathbf{k}}}{E_{\mathbf{k}}} \tanh \frac{\beta E_{\mathbf{k}}}{2} \quad (11)$$

and

$$\Delta = \frac{g_c}{L} \sum_{\mathbf{k}} d_{\mathbf{k}} \frac{\Delta_{\mathbf{k}}}{2E_{\mathbf{k}}} \tanh \frac{\beta E_{\mathbf{k}}}{2}, \quad (12)$$

respectively. The condition $\partial\omega/\partial n = 0$ (at fixed μ) yields the equation determining the density

$$n = 1 - \frac{1}{L} \sum_{\mathbf{k}} \frac{\xi_{\mathbf{k}}}{E_{\mathbf{k}}} \tanh \frac{\beta E_{\mathbf{k}}}{2}. \quad (13)$$

III. RESULTS

We now show results obtained from a numerical solution of the mean-field equations. For the ratio of hopping amplitudes we choose $t'/t = -1/6$. The bare dispersion $\epsilon_{\mathbf{k}}^0$ has saddle points at $\mathbf{k} = (\pi, 0)$, $(0, \pi)$, leading to a logarithmic van Hove singularity in the bare density of states at $\epsilon = -4t' = -2t/3$. All the results presented in the figures are for $u = 0$ (no uniform contribution to forward scattering), but we will discuss the effects of a finite u in the text. In the following we set $t = 1$, that is, all results with dimension of energy are in units of t .

In Fig. 1 we show the transition temperature $T_f(\mu)$ for Fermi surface symmetry breaking in the absence of pairing ($\Delta = 0$) for $g_f = 1$, and the critical temperature for superconductivity $T_c(\mu)$ in the absence of Fermi surface symmetry breaking ($\eta = 0$) for various choices of g_c . As discussed in detail in Refs. 15 and 16, a symmetry-broken Fermi surface is stabilized below a dome-shaped transition line, with a maximal transition temperature near van Hove filling. The transition is first order at the edges of the transition line and second order around its center. The critical temperature for superconductivity is also maximal near van Hove filling, but $T_c(\mu)$ remains finite for any μ (as long as the band is partially filled), and the transition is always of second order. Near van Hove filling the transition temperatures T_f and T_c are of the same order of magnitude for g_c slightly above $g_f = 1$. Note that in the weak coupling limit one would obtain $T_f \ll T_c$ for comparable g_f and g_c , since $\log(1/T_f) \propto g_f^{-1}$ for $g_f \rightarrow 0$,¹⁶ while $\log(1/T_c) \propto g_c^{-1/2}$ for $g_c \rightarrow 0$ at van Hove filling, due to the logarithmic divergence of the density of states, and the additional logarithm in the Cooper channel, as can be seen from the gap equation (12).

We now discuss results for the full mean-field model, allowing also for coexistence of the two order parameters. In Fig. 2 we show the low temperature region of the phase diagram in the (μ, T) -plane for $g_f = 1$ and a relatively weak BCS coupling, $g_c = 0.7$. Fermi surface symmetry breaking suppresses T_c and remains essentially unaffected by the (relatively small) superconducting gap. The suppression of T_c occurs since Fermi surface symmetry breaking splits the van Hove singularity, reducing thus the density of states at the Fermi level. However, superconductivity cannot be eliminated completely, since a logarithmic Cooper singularity survives for any reflection invariant Fermi surface. The phase diagram thus exhibits three types of first order transitions between phases with a symmetric and a symmetry-broken Fermi surface: between two normal states, between a superconductor and a normal state, and between two superconducting states. Continuing the (then metastable) phase with a symmetric Fermi surface beyond the first order transition line leads to a diverging d -wave compressibility at the fictitious second order transition line “ $T_f^{2\text{nd}}$ ” also shown in the plot.

For larger g_c the energy scale for superconductivity (gap and T_c) increases, and effects of the superconducting gap on Fermi surface symmetry breaking become more pronounced,

see Fig. 3 (here $g_c = 0.9$). In particular the first order transition line $T_f(\mu)$ is shifted toward the center of the symmetry-broken region, and approaches the fictitious second order line “ T_f^{2nd} ”. In Fig. 4 we show the Δ -dependence of the “reduced” Landau energy $\omega(\Delta) = \omega[\eta_{\min}(\Delta), \Delta] - \omega[\eta_{\min}(0), 0]$ for two points in the phase diagram which are close to each other, but on opposite sides of the first order transition between a superconducting state with a symmetric Fermi surface and a normal state with Fermi surface symmetry breaking; $\eta_{\min}(\Delta)$ minimizes $\omega(\eta, \Delta)$ for fixed Δ . Note that η_{\min} is zero for large Δ ; the kink in $\omega(\Delta)$ is due to the discontinuous onset of η for small Δ . The μ -dependence of the order parameters η and Δ is shown for various temperatures in Fig. 5. The jump of η at the first order transition induces a counter jump of Δ . For high T , superconductivity is suppressed completely by Fermi surface symmetry breaking (Fig. 5c), while for lower temperatures coexistence of the order parameters Δ and η is realized (Figs. 5a and 5b). The temperature dependence of the order parameters is shown for $\mu = -0.7$ (near van Hove filling) in Fig. 6. The increasing superconducting gap Δ leads to a decrease of η upon lowering the temperature below T_c . Superconductivity smears the single particle states over an energy range of order Δ , and thus suppresses the energy gain from a Fermi surface deformation. Fermi surface symmetry breaking is thus suppressed by the superconducting gap.

Although the system is not critical at the first order transition from a symmetric to a symmetry-broken Fermi surface, it is close to criticality in the sense that the d -wave compressibility κ_d is strongly enhanced by the forward scattering interaction. For the case of pure forward scattering (f-model) this was shown already in Ref. 16. In the presence of superconductivity with a gap function $\Delta_{\mathbf{k}}$, the d -wave compressibility is given by

$$\kappa_d = \frac{\kappa_d^0}{1 - g_f \kappa_d^0}, \quad (14)$$

where

$$\kappa_d^0 = \frac{1}{L} \sum_{\mathbf{k}} d_{\mathbf{k}}^2 \left[\frac{\beta \xi_{\mathbf{k}}^2}{2E_{\mathbf{k}}^2} \frac{1}{(\cosh \frac{\beta E_{\mathbf{k}}}{2})^2} + \frac{|\Delta_{\mathbf{k}}|^2}{E_{\mathbf{k}}^3} \tanh \frac{\beta E_{\mathbf{k}}}{2} \right] \quad (15)$$

is the d -wave compressibility in the superconducting state in the absence of forward scattering ($g_f = 0$). The enhancement of κ_d due to g_f is thus given by the “Stoner factor” $S = (1 - g_f \kappa_d^0)^{-1}$. In Fig. 7 we plot the inverse Stoner factor S^{-1} along the right first order transition line (approached from the symmetric phase) up to the tricritical temperature T_f^{tri} for various choices of g_c . It becomes clear that S is enhanced significantly by superconductivity at low temperatures. In particular, for $g_c = 0.9$ the system is very close to criticality.

Enhancing g_c beyond $g_c = 0.9$, the first order transition lines between the states with symmetric and symmetry-broken Fermi surfaces are successively replaced by a continuous phase transition. In Fig. 8 we show the phase diagram for $g_c = 1$. Here Fermi surface

symmetry breaking occurs via a continuous transition at the lowest temperatures, well below T_c . In particular, there is a continuous quantum phase transition at $T = 0$. The first order lines are connected to continuous transition lines both at the high and low temperature ends. The low temperature ends are tricritical points, where the quadratic and the quartic coefficient of the reduced Landau energy $\omega(\eta) = \omega[\eta, \Delta_{\min}(\eta)]$ both vanish. By contrast, at the high temperature ends the quartic coefficient of $\omega(\eta)$ jumps from a negative to a positive value. This discontinuity is due to the onset of Δ below T_c . Note that the high temperature ends are close to the tricritical points found for smaller g_c , such that a small jump of the quartic coefficient can turn its sign. For $g_c = 1.12$ the first order transition has disappeared completely from the phase diagram (see Fig. 9), and the transition between symmetric and symmetry-broken Fermi surfaces is always continuous. The transition lines for Fermi surface symmetry breaking and superconductivity intersect in tetracritical points, where both quadratic coefficients of $\omega(\eta, \Delta)$ vanish. Enhancing g_c further leads to a progressive suppression of Fermi surface symmetry breaking, in particular at lower temperatures, where the superconducting gap is getting large. For $g_c = 1.2$, Fermi surface symmetry breaking is eliminated completely by superconductivity at low T , while it still survives in a small region at intermediate temperatures, see Fig. 10. For even larger g_c the region with a symmetry-broken Fermi surface shrinks further until it disappears completely from the phase diagram.

Adding a uniform contribution $u > 0$ to $f_{\mathbf{k}\mathbf{k}'}$, Eq. (4), leads to a suppression of first order transitions into a phase with a symmetry-broken Fermi surface, making thus continuous transitions easier. This trend was already observed and explained in detail for the case of pure forward scattering.¹⁶ For small g_c , the tricritical points are shifted to lower temperatures by a finite u , and the first order transition line moves closer to the fictitious second order transition. The gradual replacement of the first order line by a second order for increasing g_c is accelerated for $u > 0$. For example, for $g_f = 1$, $u = 10$, and $g_c = 0.9$ the phase diagram looks qualitatively as the one in Fig. 9, with Fermi surface symmetry breaking always occurring via a continuous transition.

The (effective) interaction resulting from the Hubbard or t - J model contains also an s -wave component in the Cooper channel. In case of coexistence of superconductivity with a d -wave Fermi surface deformation, this leads to a small s -wave contribution to the gap function $\Delta_{\mathbf{k}}$, in addition to the dominant d -wave term.^{2,13}

IV. CONCLUSIONS

We have solved a mean-field model for itinerant electrons moving on a square lattice with two types of interactions: an interaction in the forward scattering channel favoring a d -wave shaped symmetry-breaking Fermi surface deformation and a reduced BCS interaction with d -wave symmetry. Making different choices for the interaction parameters, a

rich variety of possible phase diagrams has been found.

For pure forward scattering Fermi surface symmetry breaking occurs typically via a first order transition at low temperatures.^{15,16} The presence of superconductivity reduces the first order character of this transition and, if strong enough, can turn it into a continuous one. This gives rise to a quantum critical point within the superconducting phase. The superconducting gap tends to suppress Fermi surface symmetry breaking. For a certain choice of parameters one finds reentrant behavior, where Fermi surface symmetry breaking is stabilized at intermediate temperatures, while it is suppressed by the pairing gap at low temperatures. If superconductivity is too strong, Fermi surface symmetry breaking disappears completely from the phase diagram.

In microscopic models the relative strength of forward scattering and pairing interactions is determined by the microscopic interactions. In the t - J model slave-boson mean-field² and variational Monte Carlo¹⁰ calculations show that pairing prevents Fermi surface symmetry breaking, but there are strongly enhanced correlations indicating that the model is close to a d -wave Pomeranchuk instability.¹¹ This corresponds to the case of a relatively large g_c in our phenomenological mean-field model. In the weakly interacting Hubbard model coexistence of superconductivity and Fermi surface symmetry breaking has been found around van Hove filling at $T = 0$ within second order perturbation theory.¹³ The available numerical results indicate that Fermi surface symmetry breaking occurs via a continuous transition in this case, as in the phase diagrams in Figs. 8 or 9.

It would clearly be interesting to analyze how order parameter fluctuations modify the mean-field results. A renormalization group calculation by Vojta *et al.*¹⁹ suggests that a quantum critical point for orientational symmetry breaking in a d -wave superconductor is destabilized by fluctuations, leading possibly to a first order transition.

Acknowledgments

We thank Marijana Kirćan for a critical reading of the manuscript and for valuable comments.

¹ I. J. Pomeranchuk, Sov. Phys. JETP **8**, 361 (1958).

² H. Yamase and H. Kohno, J. Phys. Soc. Jpn. **69**, 332 (2000); **69**, 2151 (2000).

³ C. J. Halboth and W. Metzner, Phys. Rev. Lett. **85**, 5162 (2000).

⁴ I. Grote, E. Kōrding, and F. Wegner, J. Low Temp. Phys. **126**, 1385 (2002); V. Hankevych, I. Grote, and F. Wegner, Phys. Rev. B **66**, 094516 (2002).

⁵ B. Valenzuela and M. A. H. Vozmediano, Phys. Rev. B **63**, 153103 (2001).

⁶ S. A. Kivelson, E. Fradkin, and V. J. Emery, Nature **393**, 550 (1998).

- ⁷ S. A. Kivelson, I. P. Bindloss, E. Fradkin, V. Oganesyan, J. M. Tranquada, A. Kapitulnik, and C. Howald, *Rev. Mod. Phys.* **75**, 1201 (2003).
- ⁸ V. Hinkov, S. Pailhès, P. Bourges, Y. Sidis, A. Ivanov, A. Kulakov, C. T. Lin, D. P. Chen, C. Bernhard, and B. Keimer, *Nature* **430**, 650 (2004).
- ⁹ H. Yamase and W. Metzner, *Phys. Rev. B* **73**, 214517 (2006).
- ¹⁰ B. Edegger, V. N. Muthukumar, and C. Gros, *Phys. Rev. B* **74**, 165109 (2006).
- ¹¹ H. Yamase, *Phys. Rev. Lett.* **93**, 266404 (2004).
- ¹² C. Honerkamp, M. Salmhofer, and T. M. Rice, *Eur. Phys. J. B* **27**, 127 (2002).
- ¹³ A. Neumayr and W. Metzner, *Phys. Rev. B* **67**, 035112 (2003).
- ¹⁴ H.-Y. Kee, E. H. Kim, and C.-H. Chung, *Phys. Rev. B* **68**, 245109 (2003).
- ¹⁵ I. Khavkine, C.-H. Chung, V. Oganesyan, and H.-Y. Kee, *Phys. Rev. B* **70**, 155110 (2004).
- ¹⁶ H. Yamase, V. Oganesyan, and W. Metzner, *Phys. Rev. B* **72**, 035114 (2005).
- ¹⁷ W. Metzner, D. Rohe, and S. Andergassen, *Phys. Rev. Lett.* **91**, 066402 (2003).
- ¹⁸ L. Dell'Anna and W. Metzner, *Phys. Rev. B* **73**, 045127 (2006); cond-mat/0611723.
- ¹⁹ M. Vojta, Y. Zhang, and S. Sachdev, *Phys. Rev. Lett.* **85**, 4940 (2000); *Int. J. Mod. Phys. B* **14**, 3719 (2000).

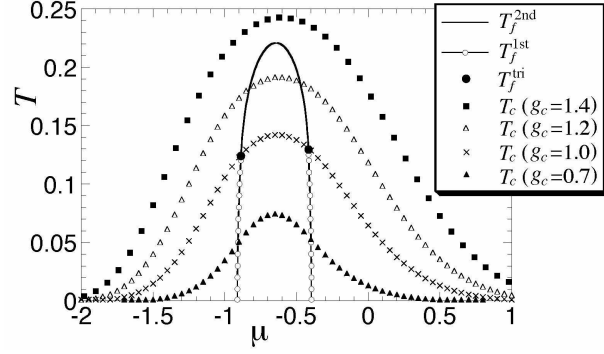


FIG. 1: Critical temperature $T_f(\mu)$ for Fermi surface symmetry breaking in the absence of superconductivity ($\Delta = 0$) for $g_f = 1$ and critical temperature for superconductivity $T_c(\mu)$ in the absence of Fermi surface symmetry breaking ($\eta = 0$) for various choices of g_c . The superconducting transition is always of second order. Fermi surface symmetry breaking occurs via a first order transition at temperatures below the tricritical points T_f^{tri} , and via a second order transition above.

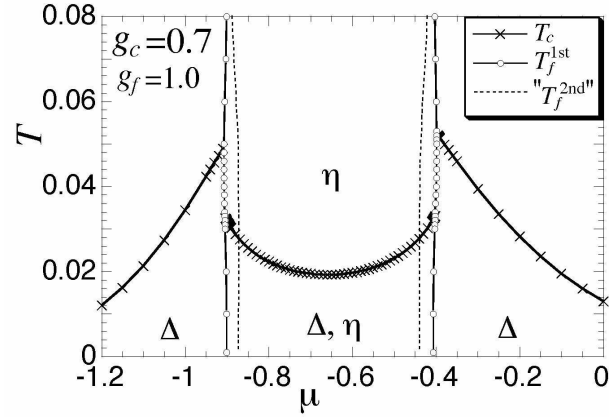


FIG. 2: Phase diagram in the (μ, T) -plane for $g_f = 1$ and $g_c = 0.7$. The symbols η and Δ indicate which order parameters are finite in the various regions confined by the transition temperatures. Fermi surface symmetry breaking occurs via a first order transition in the temperature range shown in the plot. Continuing the (then metastable) phase with a symmetric Fermi surface beyond the first order transition line leads to a diverging d -wave compressibility at the fictitious second order transition line “ T_f^{2nd} ” also shown in the plot.

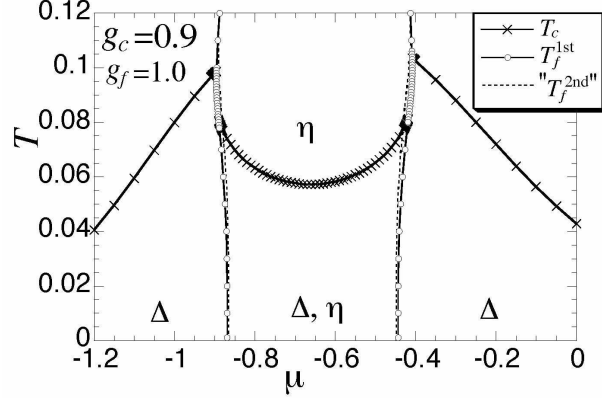


FIG. 3: Phase diagram in the (μ, T) -plane for $g_f = 1$ and $g_c = 0.9$. The first order transition line for Fermi surface symmetry breaking is very close to the fictitious second order line in this case.

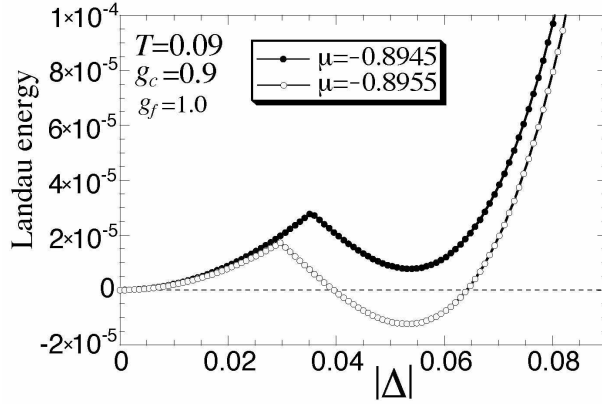


FIG. 4: Reduced Landau energy $\omega(\Delta) = \omega[\eta_{\min}(\Delta), \Delta] - \omega[\eta_{\min}(0), 0]$, minimized with respect to η , as a function of $|\Delta|$. The interaction parameters are $g_f = 1$ and $g_c = 0.9$ as in Fig. 3, the temperature is $T = 0.09$. The two choices of μ correspond to two points close to but on opposite sides of the first order transition line between a superconducting state with a symmetric Fermi surface and a normal state with a d -wave deformed Fermi surface.

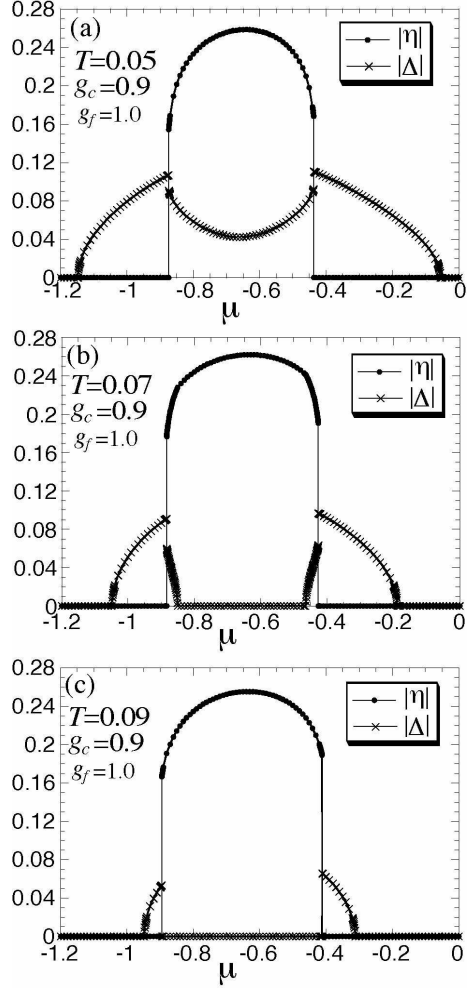


FIG. 5: Order parameters η and Δ as a function of μ for various temperatures, $T = 0.05, 0.07, 0.09$. The interaction parameters are $g_f = 1$ and $g_c = 0.9$ as in Fig. 3.

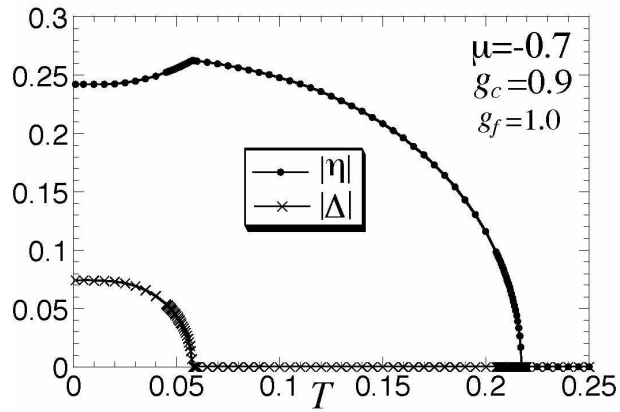


FIG. 6: Temperature dependence of the order parameters η and Δ for $\mu = -0.7$ and interaction parameters as in Fig. 3.

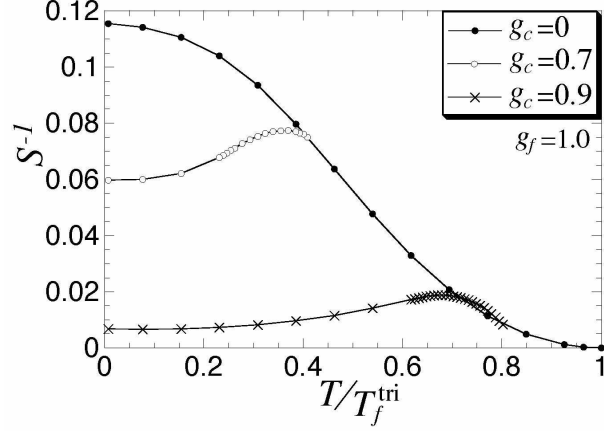


FIG. 7: Temperature dependence of the inverse Stoner enhancement of the d -wave compressibility along the right first order transition line between the phases with symmetric and symmetry-broken Fermi surface. Interaction parameters are $g_f = 1$ and $g_c = 0, 0.7, 0.9$. The tricritical point at the high temperature end of the transition line ($T_f^{\text{tri}} = 0.130$) is the same in all cases.

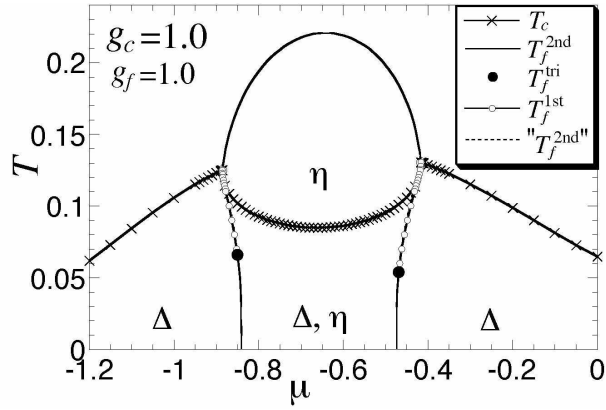


FIG. 8: Phase diagram in the (μ, T) -plane for $g_f = 1$ and $g_c = 1$. The fictitious second order transition line " $T_f^{2\text{nd}}$ " is so close to the first order line $T_f^{1\text{st}}$ that it is hidden by the latter.

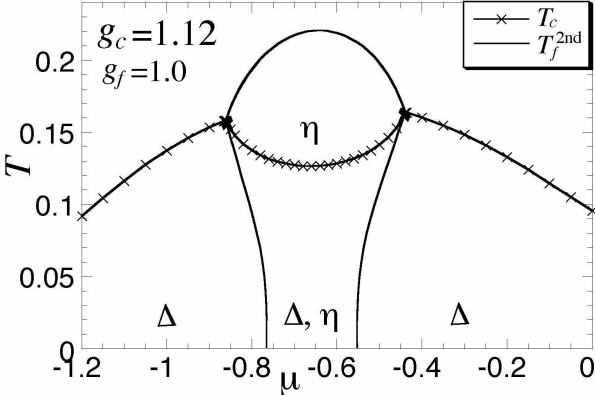


FIG. 9: Phase diagram in the (μ, T) -plane for $g_f = 1$ and $g_c = 1.12$. All transitions are of second order.

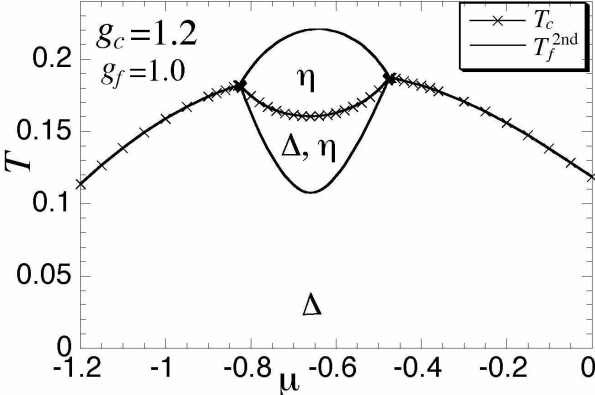


FIG. 10: Phase diagram in the (μ, T) -plane for $g_f = 1$ and $g_c = 1.2$. All transitions are of second order.